Rendiconti Lincei. Scienze Fisiche e Naturali (2021) 32:747–759
https://doi.org/10.1007/s12210-021-01016-x

RESEARCH PAPER

Evaluation of antimicrobial activities of blue-green algae-mediated silver and gold nanoparticles

Mostafa M. El-Sheekh[1] · **Lamiaa H. S. Hassan**[2] · **Hanaa H. Morsi**[2]

Received: 10 March 2021 / Accepted: 31 July 2021 / Published online: 18 August 2021

Abstract
Recently, green nanotechnology is considered a more suitable and safer tool for medical applications due to its nature reductants with low toxicity and low eco-hazard. The micro-algal biomass was used for the nanoparticles biosynthesis, depending on using whole algal cell cultivation. During the current study, cyanobacteria *Oscillatoria* sp. and *Spirulina platensis* exhibited their ability to synthesize silver oxide (Ag_2O|AgO-NPs) and gold nanoparticles (Au-NPs), respectively. The characterization results confirmed the formation of *Oscillatoria* sp.-mediated silver oxide nanoparticles (*O.*Ag_2O|AgO-NPs) and *S. platensis*-mediated gold nanoparticles (*S.*Au-NPs). Three different methods had been examined, (i) culture-free cells (secondary metabolites), (ii) algal aqueous extract, and (iii) whole cells cultivation (in vivo). UV–Vis spectroscopy confirmed the biosynthesized *O.*Ag-NPs at 438 nm, while *S.*Au-NPs reached 545 nm by whole cells cultivation technique. TEM scanning indicated the formation of spherical-shaped *O.*Ag_2O|AgO-NPs with an average size ranged between 10.49 and 45.81 nm. *S.*Au-NPs also were detected in triangular, pentagonal, and slightly spherical shapes with an average size of 15.49–55.08 nm. Both *O.*Ag_2O|AgO-NPs, and *S.*Au-NPs demonstrated antibacterial and antifungal properties against Gram-positive and Gram-negative bacteria. *S.*Au-NPs were more effective than *O.*Ag_2O|AgO-NPs, which recorded high significant MIC results against *Bacillus subtilis* ATCC 19659 (1.95 µg/ml), *Salmonella typhi* ATCC14028 (3.90 µg/ml), and *Candida tropicalis* ATCC 1380 (1.1 µg/ml) after 24 h treatment, comparing with the control. It is concluded that *O.*Ag_2O|AgO-NPs and *S.*Au-NPs have efficient antibacterial and antifungal activities.

Keywords Antibacterial · Antifungal · Green nanotechnology · Cyanobacteria · Silver nanoparticles · Gold nanoparticles

1 Introduction

Nanotechnology is a vibrant, modern, and developing branch of science that studies nanometer-scale objects, which equal a billionth from the meter (10^{-9} m) with two or more dimensions in size range between 1 and 100 nm (LewisOscar et al. 2016; Negi and Singh 2018). Nanoparticles (NPs) have unique and fascinating features that differ from their bulk material, such as changes in their physical, chemical, and biochemical properties (El-Sheekh and El-kassas 2016; El-Seedi et al. 2019).

Through the last few decades, green nanotechnology has been considered an eco-friendly approach and widely used for nanoparticles synthesis, which is preferred for medical purposes due to its no harmful effects on human health and without any risk on the environment (Jeffryes et al. 2015). This promotes nanomaterial formation biological methods, such as viruses, bacteria, algae, yeast, fungi, and plants (Pantidos and Horsfall 2014; El-Seedi et al. 2019).

Recently, algae gained wide importance in the scope of the green biosynthesis of nanoparticles (Negi and Singh 2018; Khalid 2019). Algae are a diverse collection of unicellular or multicellular autotrophic organisms of commercial and ecological value. They can be found in various environments, including freshwater, marine water, moist soil surfaces, and rocks. Microalgae and macroalgae are the two types of algae (Sharma et al. 2015a; Vincy et al. 2017; Rahman et al. 2020). Algae are considered a worthwhile source for synthesizing

✉ Mostafa M. El-Sheekh
mostafaelsheikh@science.tanta.edu.eg

[1] Department of Botany and Microbiology, Faculty of Science, Tanta University, Tanta, Egypt

[2] Department of Botany and Microbiology, Faculty of Science, Menoufia University, Menoufia, Egypt

metallic nanoparticles due to their various natural products, exuberance, and ability to accumulate metals (Ismail and Ismail 2016; Tareq et al. 2017). The metal ions reduction occurs by micro-algal activities reducing agents, such as alkaloids, carbonyl groups, flavonoids, phenols, proteins, pigments, and terpenoids (LewisOscar et al. 2016).

The proliferation and expansion of multidrug-resistant bacteria to antibiotics motivated the researchers to develop nanoparticles based on antiseptics (El-Sheekh and El-kassas 2016). The Ag-NPs option is preferred because it is non-toxic to the human body at low concentrations and has broad-spectrum antimicrobial properties (Parial et al. 2012). On various surfaces, such as catheters, Ag-NPs appear to limit bacterial colonization (Nakamura et al. 2019). The chitosan composite with Ag-NPs showed high efficiency as an antimicrobial agent that was suggested to coat the cardiovascular implants, multilayer films containing chitosan-Ag-NPs were prepared, which were effective against *Escherichia coli* (El-Sheekh and El-Kassas 2016).

Au-NPs (5 nm) synthesized by the cyanobacterium *S. platensis* showed an efficient bactericidal activity against *Bacillus subtilis* and *Staphylococcus aureus* (Suganya et al. 2015). Vancomycin-capped Au-NPs augmented the bactericidal activity against *E. coli* (Esmaeillou et al. 2017). Gold nanoparticles have also been applied in the DNA-microarray technology to identify pathogenic bacteria (Wei et al. 2018). The cyanobacterium *Microcoleus* sp.-mediated Ag-NPs (44–79 nm) showed antibacterial activities against *B. subtilis*, *E. coli*, *Proteus vulgaris*, *Salmonella typhi*, *Streptococcus* sp., *S. aureus,* and *Vibrio cholera* (Sudha et al. 2013). Pathak et al. (2019) used the cell-free extracts of cyanobacterium *Scytonema geitleri* HKAR-12 to produce Ag-NPs (9–17 nm), which exhibited bactericidal activities against *P. aeruginosa*, *E. coli* strain1, and strain 2.

Spirulina maxima-mediated Au-NPs, exhibited antifungal properties against pathogenic *Candida albicans* (*C. albicans*) with MIC 32 µg/ml (Dananjaya et al. 2020). Sonker et al. (2017) reported that Ag-NPs produced from the cyanobacterium *Nostoc* sp. strain HKAR-2 had antifungal effects against *Aspergillus niger* and *Trichoderma harzianum*. *Anabaena variabilis*-mediated Ag-NPs exhibited antifungal activities against *Candida albicans* and *Candida glabrata* (Ahamad et al. 2021).

In the light of the ability of microalgae to reduce metal ions to their nanoforms using simple requirements, the present study aims to assess the activity and efficiency of micro-algal-mediated silver oxide and gold NP as antimicrobial agents against six human pathogenic bacteria and three fungal species.

2 Materials and methods

2.1 Microalgal culture

Spirulina platensis and *Oscillatoria* sp., the two experimental blue-green algae (cyanobacteria), were isolated from freshwater canals in Shebin El-Kom City, Menoufia Government, Egypt. Healthy microalgal cultures were cultivated in semi-continuous culture on Kuhl medium at pH 9 under 60 µmol photons m^{-2} s^{-1} as a continuous illumination intensity (El-Sheekh et al. 2021).

2.2 Biosynthesis of silver and gold nanoparticles

2.2.1 Using the microalgal culture-free cells

Microalgal cells were harvested in the middle of the logarithmic phase on the 14th day and centrifuged at 4000 rpm for 15 min. The algal supernatant was stored at 4 °C for further use (Suja et al. 2016). Then, 5 ml of 200 mM $AgNO_3$ or 5 ml of 100 mM $HAuCl_4{\cdot}3H_2O$ were added slowly to 95 ml of microalgal supernatant with stirring and heating at 50 °C for 30 min using (PMC 509C Multi-Place) Magnetic Stirrer. The resulted concentrations were 10 mM $AgNO_3$ (Maria et al. 2015) and 5 mM $HAuCl_4{\cdot}3H_2O$ (El-Sheekh et al. 2020). The control solutions were prepared by adding 5 ml of 200 mM $AgNO_3$ to 95 ml distilled water and 5 ml of 100 mM $HAuCl_4{\cdot}3H_2O$ to 95 ml distilled water under the same conditions as experimental solutions. All the experiments were carried out in three replicates.

2.2.2 In vitro using microalgae aqueous extract

After removing the supernatant, the collected cells were washed with sterile distilled water five times to remove media ingredients (Senthilkumar et al. 2019). Typically, 5.0 g fresh algae were re-suspended in 100 ml of sterile distilled water and heated for 60 min at 70 °C in an Erlenmeyer flask. After that, the mixture was cooled and centrifuged at 4000 rpm for 15 min. The algal aqueous extracts were collected and stored at 4 °C till the experimental use (Sonker et al. 2017).

According to El-Sheekh and El-Kassas (2014a, b), Khalafi et al. (2019), Senthilkumar et al. (2019), the Ag-NPs and Au-NPs synthesis reactions were carried out using 5 ml of 200 mM $AgNO_3$ or 5 ml of 100 mM $HAuCl_4{\cdot}3H_2O$, respectively. They were added slowly to 95 ml of the aqueous algal extract with stirring and heating at 50 °C for 30 min.

2.2.3 In vivo using whole algal cells cultivation

Fresh biomass of *Oscillatoria* sp. and *Spirulina platensis* were used in the biosynthesis of silver oxide and gold nanoparticles, respectively, by suspending 5 g of the algal biomass in 100 ml of 10 mM, or 5 mM of an aqueous solution of $AgNO_3$ or $HAuCl_4{\cdot}3H_2O$, respectively, in a 250 ml Erlenmeyer flask (Jena et al. 2013; Soleimani and Habibi-Pirkoohi 2017). The different algae species were separately cultured along with the metal solutions and preserved in the previously described growth conditions for 24 h, according to the modified method of Merin et al. (2010). 5 g of fresh algal biomass was added to 100 ml of sterile distilled water in the control treatment. After the reaction was completed, the biomass was separated using centrifugation at 4000 rpm for 10 min. The cultured cyanobacteria were shown to be able to create nanoparticles extracellularly, release them into the solution, and reduce metallic ions intracellularly and maintain them within their cells. The intracellular production required disrupting the cells to liberate the produced nanoparticles. So, mechanical mashing of these cells using magnetic stirring at room temperature for one hour. This helped the breaking of the cells and liberation of the nanoparticles into the aqueous solution.

2.3 Characterization of the green nanoparticles

All the samples of the three nanoparticles preparation techniques were assessed by UV–Vis spectrum. Then, the best results of UV band samples were tested by the rest characterization spectra.

2.4 Ultraviolet–Visible (UV–Vis) spectrum

The resulted color changes for the bio-reduction of Ag^+ and Au^{3+} were recorded through visual observation. The UV–Vis spectra of these aliquots were investigated at 300–700 nm, using a Nano Photometer® NP80/N60/N50/C40, the Faculty of Medicine, Menoufia University Egypt. The measurements were carried out at room temperature.

2.5 X-ray diffraction (XRD) spectrum

The crystallinity and elemental content of nanoparticles were examined using XRD. The experiment was carried out at the Ecological Studies and Researches Institute, Sadat City University, Menoufia, Egypt, using an X-ray powder diffractometer (D2 PHASER 2nd Generation, Bruker AXS., Germany) with CuKá1 radiation and a programmable divergence slit, with a 40 kV voltage and a 30 mA X-ray source current.

2.6 Transmission electron microscope (TEM) scanning

Both the size and shape of nanoparticles were detected by TEM micrograph. Images were scanned on a (JEOL JEM-2100 electron microscope, Japan) with an accelerating voltage of 80 kV, Nanotechnology Centre, Egyptian Petroleum Research Institute (EPRI), Egypt. A drop of silver or gold nanoparticles solution was loaded on a carbon-coated copper grid and allowed to dry completely for an hour at room temperature. Clear microscopic views have been detected and documented in different ranges of magnification.

2.7 Antimicrobial activities of determination of the minimal inhibitory concentration (MIC) using XTT assay

The MICs were determined using the micro-dilution method described by Tunney et al. (2004) and modified by Mohammed et al. (2019). The test was investigated against human pathogenic organisms including *Staphylococcus aureus* ATCC 25923, *Bacillus subtilis* ATCC 19659 and MRSA ATCC MP-3 (Gram-positive); *Salmonella typhi* ATCC 14028, *Pseudomonas aeruginosa* ATCC 9027 and *Klebsiella pneumoniae* ATCC 70063 (Gram-negative) bacteria and *Candida albicans* ATCC 24433, *Aspergillus flavus* ATCC 9643 and *Candida tropicalis* ATCC 1380 fungi. The microbial inoculates were prepared, and the suspensions were adjusted to 10^6 CFU/mL. The samples and the standard drugs (Ciprofloxacin, Vancomycin, and Amphotericin-B) were prepared in dimethyl sulfoxide (DMSO). Then, in a 96-well plate, two-fold dilutions (125–0.48) were performed. The microplate contained 40 µl of the growth medium brain heart infusion (BHI), 10 µl of inoculum, and 50 µl of diluted samples and standard chemicals in each well. As a negative control, DMSO was utilized. The plates were incubated at 37 °C for 24 h for bacteria and unicellular fungi, while for filamentous fungi, they were incubated for 48 h. The wells were then filled with 40 µl of tetrazolium salt (2,3-bis(2-methyloxy-4-nitro-5-sulfophenyl)-2H-tetrazolium-5-carboxanilide) (XTT). Colorimetric change in the XTT reduction experiment was determined using a microtiter plate reader (Tecan Sunrise absorbance reader; Tecan UK, Reading, United Kingdom) at 492 nm after the plates were incubated in dark for 1 h at 37 °C. The percentage of inhibition was calculated using the following equation:

$$\text{Inhibition } \% = (1 - \text{Absorbance of test}/\text{Absorbance of control}) \times 100.$$

The concentration of samples (inhibitors) required for 90% inhibition (MIC_{90}) was determined from corresponding dose–response curves. The MIC was taken to the lowest concentration, with 100 inhibitory %.

2.8 Statistical analysis

ANOVA (f) test was used for data analysis at 0.05 level using SPSS for Windows (SPSS 16) software. The results of this study were presented as a mean of three replicates ± standard deviation (SD). The least significant difference (LSD) was used to compare the statistically significant difference between means at P value ≤ 0.05.

3 Results and discussion

There are two alternative techniques for metallic nanoparticles synthesizing: the top–down technique and the bottom–up technique. The bulk materials are broken down to nanometer range using physical (mechanical) or chemical ways in the top-down approach. But these methods are very expensive, required high energy, produce environmental toxic and biohazard substances. In addition, the produced nanoparticles may have size changes only without any changes in their properties. In the bottom–up methods, atoms or molecules are assembled into molecular structures in nanosize. Bottom–up approach is the technique used in chemical and biological nanoparticles synthesizing, with very high efficiency (Kattarath and Ramani 2017; Khanna et al. 2019).

3.1 Characterization of the *O*.Ag_2O|AgO-NPs, and *S*. Au-NPs

During this study, the biosynthesis of silver and gold nanoparticles from cyanobacteria (*S. platensis* and *Oscillatoria* sp.) was done through three different methods, (i) culture-free cells (secondary metabolites), (ii) algal aqueous extract, and (iii) whole cells cultivation (in vivo). UV–Vis spectroscopy has been used as a screening technique, which gives the first confirmation on the formation of the best nanoparticles by the third method. So, we used the third method for *O*. Ag_2O|AgO-NPs, and *S*.Au-NPs biosynthesis to complete the rest of the characterization tests and the applications.

In this method, extracellular nanoparticles formation was observed in all reduction cases, except at Ag-NPs synthesis using *Oscillatoria* sp. cultivation (in vivo). The Ag-NPs were formed intracellularly, as the blue-green color of *Oscillatoria* sp. filaments converted to brown (Fig. 1). The intensity of the color increased after 24 h of incubation when *S. platensis* reduced Au^{3+} to Au-NPs extracellular with purple or ruby red color (Fig. 2) (El-Sheekh and El-Kassas 2014a, b; Adebayo-Tayo et al. 2018).

Spirulina platensis could undergo intracellular silver ions (Ag^+) reduction only by cultivation in an $AgNO_3$ medium. The λ_{max} was ranged from 374 to 460 nm, but it showed no ability to reduce Ag^+ through their secondary metabolites or aqueous extract, as shown in Fig. 3a. This agrees with El-Sheekh and El-Kassas (2014a), Patel et al. (2015), who mentioned the extracellular formation of Ag-NPs by *S. platensis*. While Muthusamy et al. (2017) reported the biosynthesis of Ag-NPs by mixing *S. platensis* aqueous extract with 1 mM $AgNO_3$. Ag-NPs peak was observed at 450 nm. The results of Fig. 3b showed the best UV–Vis spectrum peak

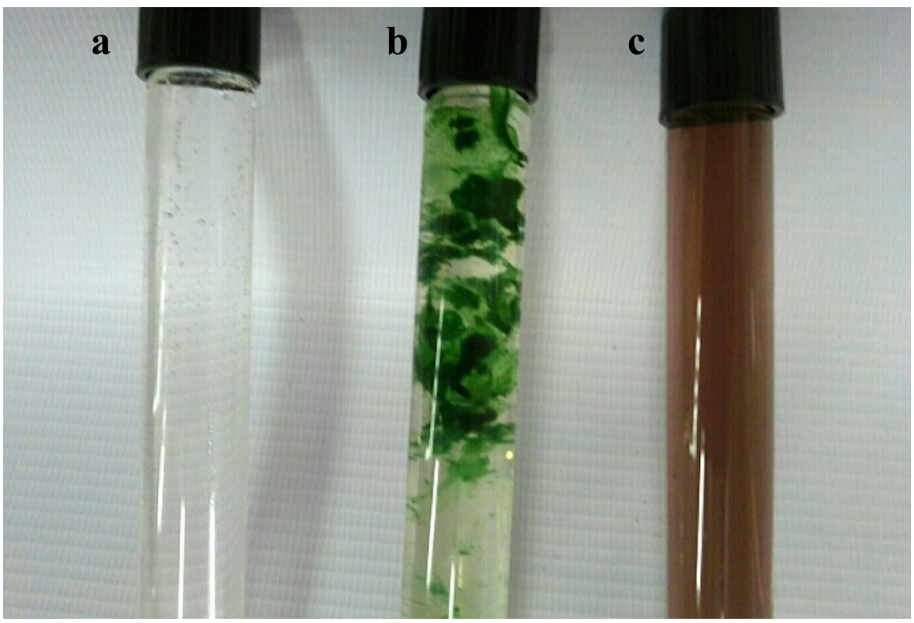

Fig. 1 **a** $AgNO_3$ solution, **b** Freshly *Oscillatoria* biomass in sterilized distilled water, and **c** *Oscillatoria* sp. mediated AgO_2|AgO-NPs

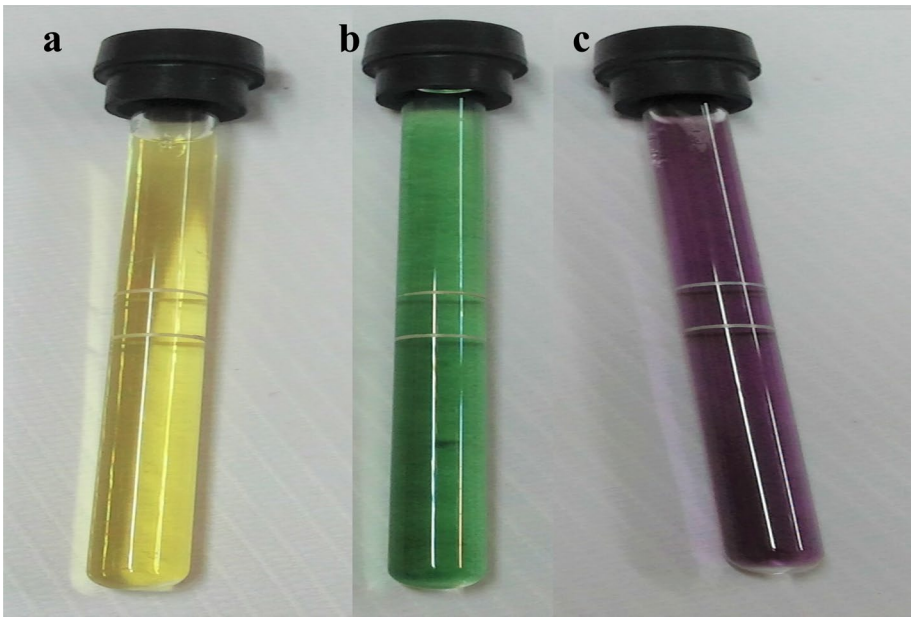

Fig. 2 **a** $HAuCl_4.3H_2O$ solution, **b** Freshly *Spirulina platensis* biomass in sterilized distilled water, and **c** *Oscillatoria* sp. mediated Au-NPs

resulted for Ag-NPs was detected at 438 nm by the intracellular reduction by the cultivation of *Oscillatoria* sp. in 10 mM $AgNO_3$ medium. *Oscillatoria* sp. exhibited no reduction by their secondary metabolites, but the aqueous extract could form Ag-NPs with a broad peak appeared by UV–Vis spectrum (450 nm). *Oscillatoria willei* NTDM01 was mentioned for their ability to biosynthesis Ag-NPs with a size range between 100 and 200 nm (Ali et al. 2011; Al-Katib et al. 2015). As Ag-NPs can be synthesized intracellularly by an enzymatic process, where the applied concentration of $AgNO_3$ was not toxic to the cultivated cells (Patel et al. 2015). According to Avilala and Golla (2019), the biosynthesis of Ag-NPs necessitates the use of a NADH-based nitrate reductase enzyme that reduces Ag^+. The results of Fig. 3c confirmed the biosynthesis of Au-NPs by the culture-free cells and the in vitro extracellular cultivation of *S. platensis*, respectively, with λ_{max} ranged around 545–560 nm. Whilst there was no formation of Au-NPs by the aqueous extract of *S. platensis*. These results agree with Khan et al. (2019), who reported the ability of *S. subsalsa* and *S. platensis* to undergo extracellular synthesizing of Au-NPs. The results differ with Suganya et al. (2015), who concluded Au-NPs formation using extract of *S. platensis*. *Oscillatoria* sp. showed no significant formation of Au-NPs (Fig. 3d). The best results were detected at 438 nm for *O.*Ag-NPs, and 545 nm *S.*Au-NPs.

Figure 4 exhibited XRD bands, which revealed the elementary and crystallinity nature of Ag_2O|AgO-NPs, and Au-NPs from the cultivation of *Oscillatoria* sp. and *S. platensis*, respectively. Sharp peaks from 0^o to $80°$ at 2θ were observed in the XRD pattern, which correlated to the Bragg's reflections in a face-centered spherical shape *O.*Ag_2O|AgO-NPs with basal 200, 111, 311, and 222. While the XRD of *S.*Au-NPs showed distinct diffraction peaks at 2θ values corresponded with 111, 200, 220, 311, and 222. The extreme peaks further confirmed triangular-shaped *S.*Au-NPs. TEM results of *O.*Ag_2O|AgO-NPs which exhibited spherical morphology with a diameter of 10.49–45.81 nm, which were quasi-spherical and well dispersed in nature, while *S.*Au-NPs demonstrated octahedral, pentagonal, and triangular-shaped nanoparticles free from any aggregation, with average particle size 15.49–55.08 nm (Fig. 5). Mahdieh et al. (2012) used XRD analysis and recorded the formation of spherical-shaped (Ag_2O or AgO) with an average size of 11.6 nm. The results also agree with Husain et al. (2015), Hamida et al. (2020). Patel et al. (2015) reported that Ag-NPs could be synthesized intracellularly by an enzymatic process, where the applied concentration of $AgNO_3$ was not toxic to the cultivated cells. *Oscillatoria willei* NTDM01 was mentioned for their ability to biosynthesis Ag-NPs with a size range between 100 and 200 nm (Ali et al. 2011; Al-Katib et al. 2015; Sharma et al. 2015b). According to the researchers, the biosynthesis of Ag-NPs necessitates the use of a NADH-based nitrate reductase enzyme to reduce Ag^+ (Roh et al. 2001; Avilala and Golla 2019). Hamouda et al. (2019) detected quasi-spherical silver NPs with size ranged between 3.3 and 17.9 nm. Another study showed that spherical-shaped silver nanoparticles' formation ranged in size from 4.5 to 26.0 nm (Hamida et al. 2020). The results are correlated to that reported by González-Ballesteros et al. (2017), Khanna et al. (2019).

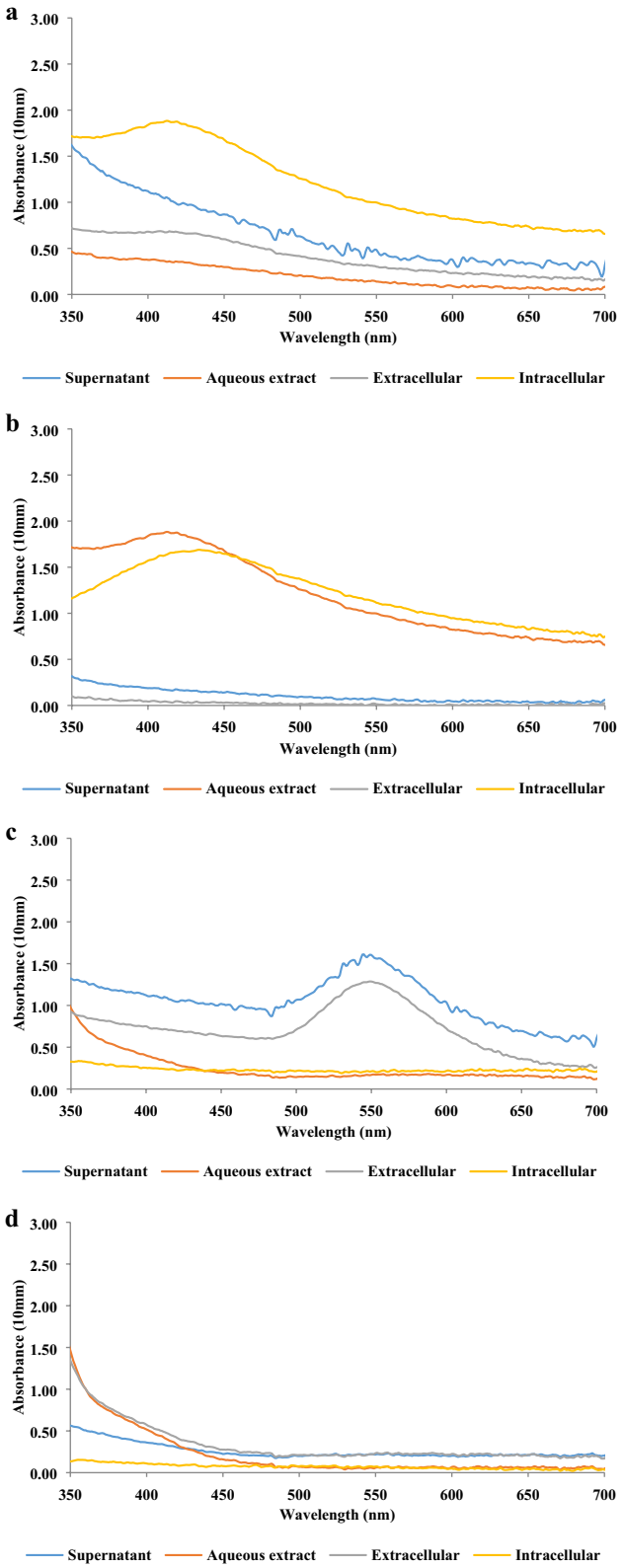

Fig. 3 UV/Vis absorption spectrum of: **a** Ag-NPs synthesized using *Spirulina platensis*; **b** Ag-NPs synthesized using *Oscillatoria* sp.; **c** Au-NPs synthesized using *S. platensis*; and **d** Au-NPs synthesized using *Oscillatoria* sp.

As shown in the authors' previous paper, El-Sheekh et al. (2020), the characterization results have demonstrated that the FTIR spectrum revealed that polysaccharides and proteins played a role in nanoparticles reduction and worked as capping agents. FTIR spectroscopy of *O.*Ag_2O|AgO-NPs, and *S.*Au-NPs exhibited the dual role of algal bio-compounds as a reducing and capping agent. Capping agents play a very important role in the stability and capping of nanoparticles (El-Sheekh and El-Kassas 2014b; Moshfegh et al. 2019). The results revealed that the algal polysaccharides, proteins, and phenolic compounds are responsible for reducing Ag^+ because proteins are characterized by the carboxylic and amine groups. Muthusamy et al. (2017) reported that protein, polysaccharides, and phenolic compounds revealed a fascinated role as stabilizing and capping agents of nanoparticles. A previous study stated the formation of Ag-NPs by *C. vulgaris*, as proteins played as a reducing agent of Ag^+ depending on the carboxyl groups in aspartate or glutamate residues and hydroxyl groups in tyrosine residues. In addition to working as a stabilizing agent (Corciova and Ivanescu 2018). Hamida et al. (2020) used *Desertifilum* IPPAS B-1220 to form silver nanoparticles and stated that polysaccharides and proteins worked as a capping agent.

It was suggested that nanoparticles formation by microalgae starts with binding, accumulation, then intracellular reduction, followed by extracellular formation (Parial and Pal 2015; Khanna et al. 2019). Abiotic components, such as reducing sugars in the polysaccharide sheath and fatty acids in the plasma membrane and other cellular reducing entities, are involved in the reduction process, biotic factors such as the involvement of reducing enzymes (Bakir et al. 2018). It was reported that during the extracellular reduction, exo-polysaccharide had been formed when parts of polysaccharides sheath may be separated from the filaments in the solution. This exopolysaccharide contains many effective reducing sugars that can form nanoparticles (Bakir et al. 2018). The synthesis of nanoparticles may depend on the concentration of metal ions in addition to the number of cells or the biologically active molecules concentration (Bakir et al. 2018). The size, shape, and distribution of nanoparticles affect their efficiency, which are controlled by synthesis procedures, reducing agents, and stabilizers. Algal pigments are rich in hydroxyl groups, which are responsible for reducing metal ions (Mata et al. 2009). For cyanobacteria, it has been suggested that the proteinaceous pigment C-phycocyanin and polysaccharides are responsible for the nanoparticles biosynthesis (Patel et al. 2015; Bakir et al. 2018). The cyanobacterial extract is rich with a variety of active compounds that may be able to reduce metal ions to nano form, for example, thiazole peptides (pseudodysidenin, nordysidenin), barbamide (mixed polypeptide–polyketide), pseudodysidenin, nordysidenin, and apramides (linear peptides), and lyngbyapeptin-A (Bakir et al. 2018).

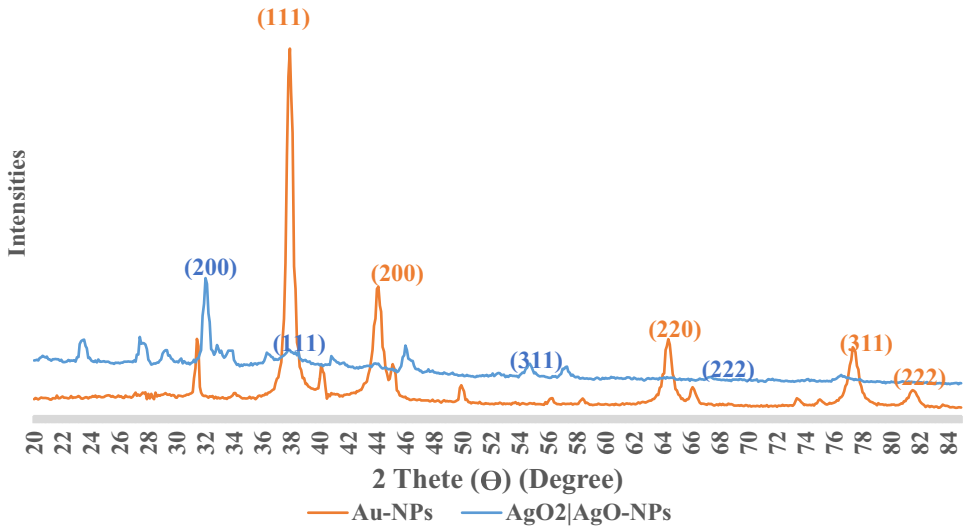

Fig. 4 X-ray diffraction (XRD) spectrum of **a** *Oscillatoria* sp. mediated *O.*AgO_2|AgO-NPs and **b** *Spirulina platensis*-mediated Au-NPs

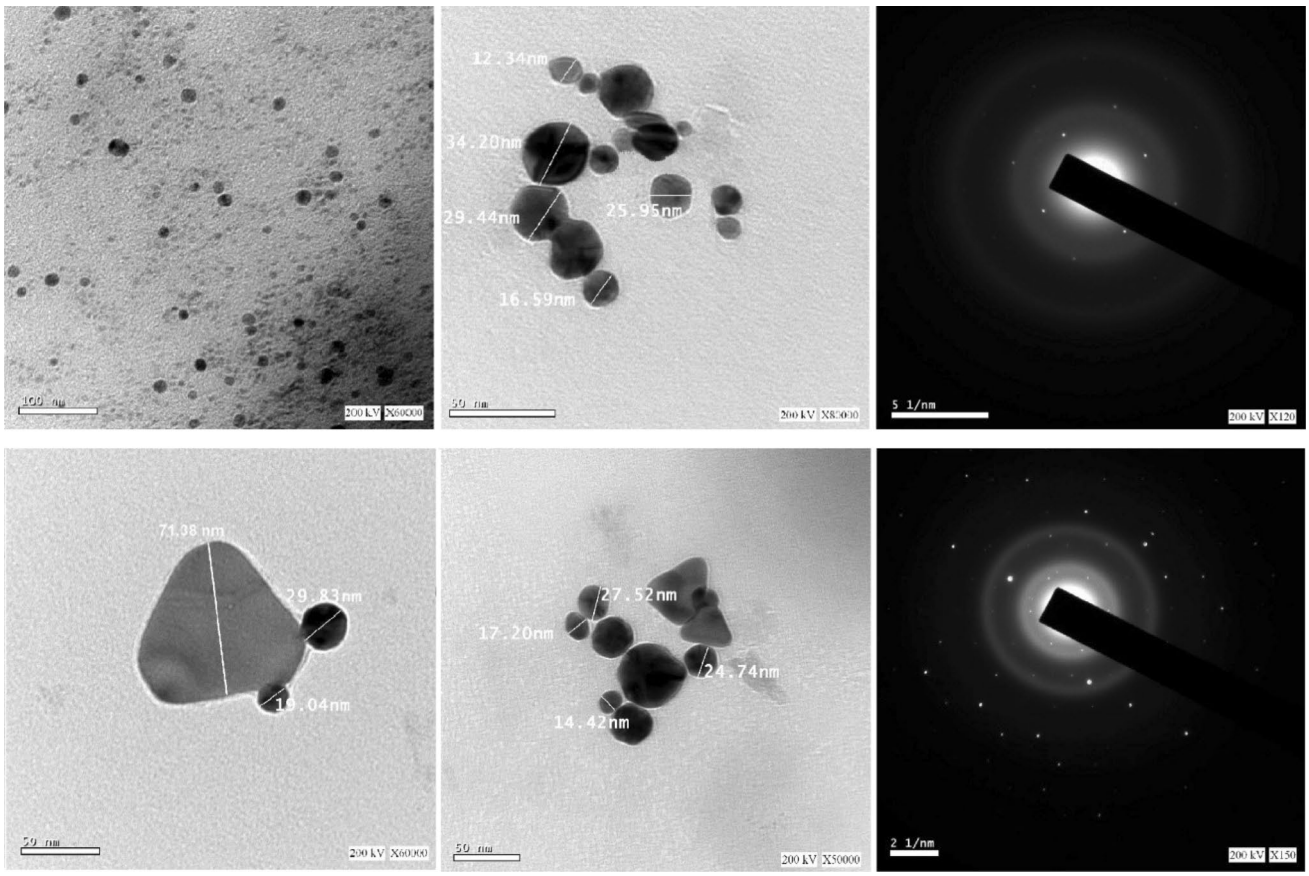

Fig. 5 Transmission electron microscope (TEM) of **a** *Oscillatoria* sp. mediated AgO_2|AgO-NPs and **b** *Spirulina platensis*-mediated Au-NPs

Table 1 Mean Inhibition concentration (MIC) of different concentrations of phytogenic Ag_2O|AgO-NPs on some pathogenic bacterial strains

	Gram-positive bacteria			Gram-negative bacteria		
Sample conc. (µg/ml)	*S. aureus* ATCC 25923	*B. subtilis* ATCC 19659	MRSA ATCC MP-3	*S. typhi* ATCC 14028	*P. aeruginosa* ATCC 9027	*K. pneumoniae* ATCC 70063
125	100 ± 00^{a}	100 ± 00^{a}	100 ± 00^{a}	100 ± 00^{a}	100 ± 00^{a}	100 ± 00^{a}
62.5	100 ± 00^{a}	100 ± 00^{a}	100 ± 00^{a}	100 ± 00^{a}	100 ± 00^{a}	100 ± 00^{a}
31.25	100 ± 00^{a}	100 ± 00^{a}	83.25 ± 4.3^{c}	100 ± 00^{a}	91.58 ± 4.5^{b}	100 ± 00^{a}
15.63	92.15 ± 3.1^{b}	100 ± 00^{a}	71.24 ± 2.9^{d}	100 ± 00^{a}	82.14 ± 3.8^{c}	100 ± 00^{a}
7.81	76.31 ± 2.5^{c}	100 ± 00^{a}	56.32 ± 2.4^{e}	87.32 ± 3.9^{b}	67.19 ± 2.9^{d}	83.24 ± 3.9^{b}
3.9	49.32 ± 2.4^{c}	83.25 ± 3.3^{a}	22.86 ± 1.5^{d}	59.32 ± 2.7^{b}	49.32 ± 2.3^{c}	56.32 ± 2.7^{b}
1.95	18.35 ± 1.3^{d}	69.32 ± 2.8^{a}	9.32 ± 0.8^{e}	38.35 ± 1.7^{b}	31.08 ± 1.7^{c}	32.16 ± 1.9^{c}
0.98	6.32 ± 0.7^{d}	56.31 ± 2.1^{a}	0.00^{e}	10.63 ± 0.9^{c}	19.35 ± 0.9^{b}	19.32 ± 1.0^{b}
0.48	0.00^{d}	21.32 ± 1.1^{a}	0.00^{d}	0.00^{d}	6.32 ± 0.3^{c}	9.31 ± 0.6^{b}
0	0.00^{a}	0.00^{a}	0.00^{a}	0.00^{a}	0.00^{a}	0.00^{a}
MIC_{90} (µg/ml)	**11.7**	**4.4**	**35.1**	**7.6**	**22.9**	**8.7**
MIC (µg ml)	**31.25**	**7.81**	**62.5**	**15.63**	**62.5**	**15.63**
Ciprofloxacin MIC (µg/ml)	**1.95**	**0.98**	**–**	**1.95**	**3.9**	**1.95**
Vancomycin MIC (µg/ml)	**–**	**–**	**3.9**	**–**	**–**	**–**

Bold indicates the final results of the test, which show the MIC and MIC90 of the tested nanoparticles when compared with the positive control Ciprofloxacin and Vancomycin

All determinations were carried out in triplicate manner and values are expressed as the mean ± SD. The MIC value is defined as the lowest concentration to inhibit 100% of microbial growth under the assayed conditions

a, b, c, d and e: there is no significant difference ($P > 0.05$) between any two groups, within the same row having the same superscript letter

3.2 Antimicrobial activities of the *O*.Ag_2O|AgO-NPs, and *S*.Au-NPs

3.2.1 Antibacterial activities

Table 1 revealed the antibacterial effect of *O*.Ag_2O|AgO-NPs, which exhibited that at concentrations 125 and 62.5 µg/ml, there was complete inhibition to all included Gram-positive and Gram-negative bacteria. At 31.25 µg/ml, there was partial inhibition of *P. aeruginosa* and MRSA, and the inhibition was statistically significant higher in *P. aeruginosa* than MRSA. *P. aeruginosa*, MRSA, and *S. aureus* were partially inhibited at 15.63 µg/ml of the sample, and there was statistically significant difference between them, while *S. aureus* was the highest then *P. aeruginosa,* then MRSA. At 7.81 µg/ml, *P. aeruginosa*, MRSA, *S. aureus*, in addition to S. *typhi* and *K. pneumonia,* were partially inhibited, where *K. pneumoniae* and *S. typhi* were the highest with no statistically difference then *S. aureus,* then *P. aeruginosa*, then MRSA. At 3.9 µg/ml, all the bacterial species showed statistically significant differences, *B. subtilis* was the highest, then *K. pneumoniae* and *S. typhi* showed no statistically difference, then *S. aureus* and *P. aeruginosa* with no statistically difference, then MRSA. All Gram-positive and -negative bacteria were partially inhibited to a lesser degree at 1.95 µg/ml, *B. subtilis* was the highest, then *S. typhi* then *K. pneumoniae* and *P. aeruginosa* with no statistically difference then *S. aureus*, then MRSA. At 0.98 µg/ml of the sample, MRSA had total inhibition while the rest of the bacterial species were partially inhibited to less than 20% except *B. subtilis* was inhibited nearly to half. *B. subtilis* was the highest, then *S. typhi,* then *K. pneumoniae,* and *P. aeruginosa* with no statistically difference then *S. aureus*. At 0.48 µg/ml, MRSA, *S. aureus*, and S. *typhi* showed no *inhibition,* and the Gram-positive and -negative bacteria were partially inhibited to less than 10% except, *B. subtilis* was inhibited nearly to the fifth, *B. subtilis* was the highest then *K. pneumoniae*, then *P. aeruginosa* with statistically significant difference.

Although *O*.Ag_2O|AgO-NPs showed a potent inhibitory effect against *S. aureus* ATCC 25923, *B. subtilis* ATCC 19659, *S. typhi* ATCC 14028, *P. aeruginosa* ATCC 9027, and *K. pneumonia* ATCC 70063 with MIC values of 11.7, 4.4, 7.6, 22.9, 8.7 µg/ml, respectively, Ciprofloxacin was the most effective bactericidal that cause MIC 1.95, 0.98, 1.95, 3.9, and 1.95, respectively. While *O*.Ag_2O|AgO-NPs showed lower antimicrobial activities on MRSA ATCC MP-3 (MIC = 35.1 µg/ml) compared with Vancomycin (MIC = 3.9 µg/ml).

Table 2 Mean Inhibition concentration (MIC) of different concentrations of phytogenic Au-NPs on some pathogenic bacterial strains

	Gram-positive bacteria			Gram-negative bacteria		
Sample conc. (µg/ml)	*S. aureus* ATCC 25923	*B. subtilis* ATCC 19659	MRSA ATCC MP-3	*S. typhi* ATCC 14028	*P. aeruginosa* ATCC 9027	*K. pneumoniae* ATCC 70063
125	100 ± 00^{a}	100 ± 00^{a}	100 ± 00^{a}	100 ± 00^{a}	100 ± 00^{a}	100 ± 00^{a}
62.5	100 ± 00^{a}	100 ± 00^{a}	100 ± 00^{a}	100 ± 00^{a}	100 ± 00^{a}	100 ± 00^{a}
31.25	100 ± 00^{a}	100 ± 00^{a}	100 ± 00^{a}	100 ± 00^{a}	100 ± 00^{a}	100 ± 00^{a}
15.63	100 ± 00^{a}	100 ± 00^{a}	100 ± 00^{a}	100 ± 00^{a}	100 ± 00^{a}	100 ± 00^{a}
7.81	100 ± 00^{a}	100 ± 00^{a}	90.14 ± 5.5^{b}	100 ± 00^{a}	86.34 ± 5.1^{b}	100 ± 00^{a}
3.9	86.32 ± 4.7^{b}	100 ± 00^{a}	76.38 ± 4.0^{c}	100 ± 00^{a}	61.32 ± 3.7^{d}	92.15 ± 5.3^{b}
1.95	62.14 ± 3.6^{c}	100 ± 00^{a}	49.32 ± 3.1^{d}	86.35 ± 4.0^{b}	46.47 ± 2.2^{d}	63.24 ± 3.7^{c}
0.98	32.16 ± 2.0^{d}	89.32 ± 5.0^{a}	$28.31 \pm 1.4^{d,e}$	69.14 ± 2.3^{b}	26.89 ± 1.7^{e}	49.32 ± 2.9^{c}
0.48	$19.32 \pm 1.4^{c,d}$	63.25 ± 2.8^{a}	9.34 ± 0.6^{e}	51.25 ± 1.9^{b}	17.35 ± 0.8^{d}	21.32 ± 1.8^{c}
0	0.00^{a}	0.00^{a}	0.00^{a}	0.00^{a}	0.00^{a}	0.00^{a}
MIC_{90} (µg/ml)	**3.9**	**0.8**	**6.23**	**1.9**	**7.9**	**3**
MIC (µg ml)	**7.81**	**1.95**	**15.63**	**3.9**	**15.63**	**7.81**
Ciprofloxacin MIC (µg ml)	**1.95**	**0.98**	**–**	**1.95**	**3.9**	**1.95**
Vancomycin MIC (µg ml)	**–**	**–**	**3.9**	**–**	**–**	**–**
Amphotericin-B MIC (µg ml)	**–**	**–**	**–**	**–**	**–**	**–**

Bold indicates the final results of the test, which show the MIC and MIC90 of the tested nanoparticles when compared with the positive control Ciprofloxacin and Vancomycin

All determinations were carried out in triplicate manner and values are expressed as the mean ± SD. The MIC value is defined as the lowest concentration to inhibit 100% of microbial growth under the assayed condition

a, b, c, d and e: there is no significant difference ($P > 0.05$) between any two groups, within the same row having the same superscript letter

Table 2 showed that *S*.AuNPs showed better antimicrobial activities than *O*.Ag_2O|AgO-NPs. For Gram-positive bacteria, the best MIC_{90} results of Au-NPs were found for *B. subtilis* ATCC 19659 (0.80 µg/ml) and followed by *S. aureus* ATCC 25923 (3.90 µg/ml). Au-NPs also revealed a good bactericidal effect against MRSA ATCC MP-3 with MIC_{90} (6.23 µg/ml), while the MIC for Vancomycin as a positive control was 1.40 µg/ml. For Gram-negative bacteria, *S*.Au-NPs also showed a very optimistic antimicrobial activities, their MIC_{90} recorded 1.90, 3.00, and 7.90 µg/ml, respectively, for *S, typhi* ATCC 14028, *K pneumoniae* ATCC 70063, and *P aeruginosa* ATCC 9027. At 125, 62.5, 31.25 and, 15.63 µg/ml, there was complete inhibition to all included Gram-positive and Gram-negative bacteria. While there was partial inhibition of *P. aeruginosa* and MRSA at 7.81 µg/ml, and the inhibition was slightly higher in MRSA than *P. aeruginosa* with no statistically significant difference. At 3.9 µg/ml, *S. aureus* and *K. pneumonia* in addition to *P. aeruginosa*, and MRSA were partially inhibited, where *S. aureus* and *K. pneumonia* were the highest with no statistically significant difference then MRSA, then *P. aeruginosa.* At 1.95 µg/ml, there was statistically significant difference between *P. aeruginosa*, MRSA, *S. aureus*, *and K. pneumoniae* in addition to S. *typhi*, at which *S. typhi* was the highest, followed by *S. aureus,* but *K. pneumoniae* showed no statistically difference as well as MRSA, and P. *aeruginosa*. A partial inhibition of *B. subtilis*, *P. aeruginosa*, MRSA, *S. aureus*, S. *typhi*, and *K. pneumonia* appeared at 0.98 µg/ml, at which *B. subtilis* was the highest then *S. typhi* then *K. pneumoniae*, then *S. aureus* then MRSA and *P. aeruginosa* with no statistically difference. At 0.48 µg/ml, *B. subtilis*, *P. aeruginosa*, MRSA, *S. aureus*, S. *typhi,* and *K. pneumonia* were partially inhibited discerningly, and there was statistically significant difference between them, *B. subtilis* was the highest then *S. typhi* then *K. pneumoniae* then *S. aureus* then *P. aeruginosa*, then MRSA.

Significant results were obtained by Muthusamy et al. (2017), who reported the bactericidal effect of cyanobacteria-mediated Ag-NPs against *Staphylococcus* sp. and *Klebsiella* sp. Hamida et al. (2020) reported the same result since they tested the antibacterial activities of Ag-NPs against *B. cereus* and *B. subtilis,* and they found that streptomycin showed the best results. Sonker et al. (2017) also reported the antibacterial activities of Ag-NPs synthesized by *Nostoc* sp. strain HKAR-2 against *Ralstonia solanacearum Xanthomonas campestris*. *S*.Au-NPs also revealed

a good bactericidal effect against MRSA ATCC MP-3 with MIC90 (6.23 µg/ml), while the MIC for Vancomycin as a positive control was 1.40 µg/ml. For Gram-negative bacteria, *S.*Au-NPs also showed a very optimistic antimicrobial activities, their MIC90 recorded 1.90, 3.00, and 7.90 µg/ml, respectively, for *S, typhi* ATCC 14028, *K pneumoniae* ATCC 70063, and *P aeruginosa* ATCC 9027. In addition to this, Fig. 7 showed that Au-NPs antifungal activities against three pathogenic fungi, *Candida tropicalis* ATCC 1380, *C. albicans* ATCC 24433, and *Aspergillus flavus* ATCC 9643, with MIC90 1.10, 2.90, and 6.20 µg/ml, respectively. The MIC90 results for the positive control (Amphotericin-B) recorded 0.40, 0.70, and 2.30 µg/ml, respectively.

Different scenarios illustrate the behaviors of nanoparticles versus bacterial cells. Sharma et al. (2015b) suggested that Ag-NPs can form free radicals responsible for their antimicrobial activities. Additionally, the reactive oxygen species (ROS) may cause the breakdown of membrane function, increased cell membrane permeability or cell material leakage, morphological changes of bacterial cells, and growth inhibition. They also reported the attraction between the negative charged bacterial cell wall and the weak positive charged nanoparticles, which depended on the nanoparticles concentration and the large surface area of nanoparticles. The cytoplasmic content is released to the medium, leading to cell death. In addition, Ag-NPs showed an interaction with the thiol groups of bacterial proteins and may damage DNA replication, while large nanoparticles cannot penetrate the microbial cell and cause a less inhibitory effect (Kattarath and Ramani 2017). Another study reported that 20 nm Ag-NPs could penetrate the bacterial cell by attaching to the sulfur-containing protein of bacterial cell membrane, which causes an increase in membrane permeability and cell death (Morones et al. 2005; El-Sheekh and El-Kassas 2016). Cui et al. (2012) stated that Au-NPs could change the membrane potential and stop ATP synthase activities from decreasing the ATP level, indicating a general decline in metabolism. They can also prevent the subunit of the ribosome for RNA binding, indicating a biological process collapse. Nanoparticles have high efficiency as antimicrobial agents due to their small size that allows penetration of cellular membranes. They can cause disorders in cellular functions, including membrane permeability, respiratory activity, and DNA replication (Bakir et al. 2018). Due to their antibacterial properties and ability to remove waste materials from the skin and manage sebum, gold NPs inhibited a variety of Gram-positive and Gram-negative bacteria and fungi, increasing their esthetic and industrial benefits against acne or scurf (Bakir et al. 2018). Poulose et al. (2014) reported that the antimicrobial activity of Ag-NPs was size-dependent, as the smaller particles were more effective against many pathogens than the larger ones (Muthusamy et al. 2017). Some reports discussed the Ag-NPs mode of action against *E. coli*, as nanoparticles made pores in the bacterial cell wall and increased membrane permeability, inactivating the cell activity and causing cell death (Beyth et al. 2015). Other researchers revealed that Ag-NPs adhere to the bacterial wall and penetrate the membrane inside the microbial cell. The nanoparticles made bonds with the carboxyl, thiol, and amino groups of the biomolecules (proteins, lipids, and DNA). This causes protein disruption, intracellular biological functions inhibition, and cell death (Qing et al. 2018).

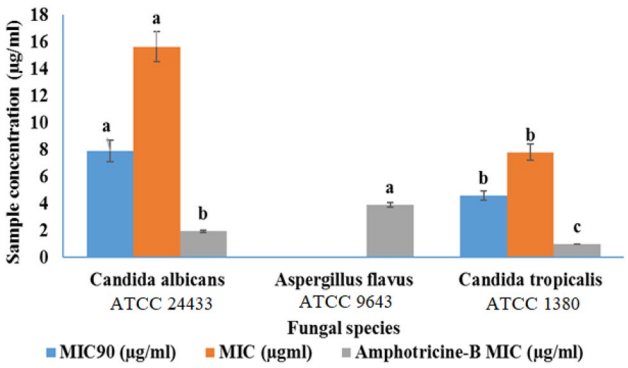

Fig. 6 Mean Inhibition concentration (MIC) of different concentrations of phytogenic *O.*AgO_2|AgO-NPs on some pathogenic fungal strains

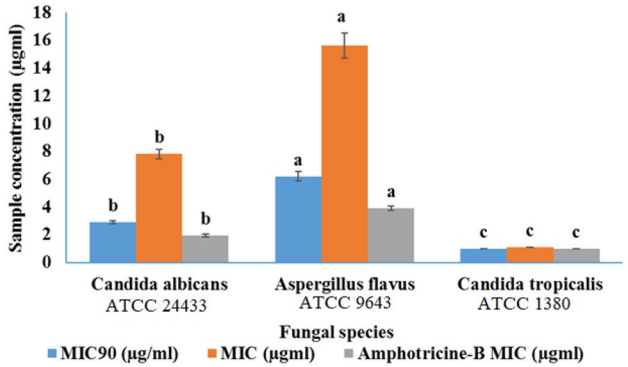

Fig. 7 Mean Inhibition concentration (MIC) of different concentrations of phytogenic *S.*Au-NPs on some pathogenic fungal strains

3.2.2 Antifungal activities

O.Ag_2O|AgO-NPs exhibited antifungal activities against two yeast species *Candida tropicalis* ATCC 1380 and *C. albicans* ATCC 24433 with MIC_{90} 4.60 and 7.90 µg/ml, which were compared with Amphotericin-B as a positive control which recorded 1.95, and 0.98 µg/ml (Fig. 6). The comparison between fungal species demonstrated that *O.*Ag_2O|AgO-NPs had no inhibitory effect against *A. flavus* ATCC 9643. This means that *O.*AgO_2|AgO-NPs could not affect the filamentous fungal forms. There was a statistically significant

difference between species regarding Amphotericin-B MIC, where *A. flavus* ATCC 9643 was the highest, then *C. albicans* ATCC 24433, then *C. tropicalis* ATCC 1380.

The results of *S.*Au-NPs have been revealed their growth inhibition against yeasts as well as fungi. As shown in Fig. 7, *S.*Au-NPs exhibited efficient effects against *C. tropicalis* ATCC 1380, *C. albicans* ATCC 24433, and *A. flavus* ATCC 9643, with MIC_{90} 1.10, 2.90, and 6.20 µg/ml, respectively. The MIC_{90} results for the positive control (Amphotericin-B) recorded 0.40, 0.70, and 2.30 µg/ml, respectively. The results were statistically significant higher in *A. flavus* ATCC 9643 than both *Candida* spp., and the MIC90 and MIC of sample two and Amphotericin-B MIC of *C. albicans* ATCC 24433 statistically significantly higher than *C. tropicalis* ATCC 1380.

Ag-NPs were found to have antifungal properties because they produced insoluble compounds by inactivating sulfhydryl groups in the fungal cell wall and disrupting membrane-bound enzymes and lipids, resulting in cell lysis. Nano-silver is effective against yeast-like fungi (El-Sheekh and El-Kassas 2016). Dnyaneshwar and Mulani (2019) stated the effectively antifungal effect of Au-NPs against the biofilms of *C. albicans*. Yu et al. (2016) reported that Au-NPs could inhibit the growth, reduce the adhesion, and stop developing *C. albicans* biofilm with MIC value of 63.38 µg/ml. It was reported that *Spirulina maxima* mediated Au-NPs against the pathogenic yeast *C. albicans*, which recorded MIC 32 µg/ml, as it was observed that Au-NPs caused damage on the cell wall of *C. albicans* and increasing the membrane permeability, and led to cell death (Dananjaya et al. 2020).

4 Conclusion

Biogenic silver oxide and gold nanoparticles mediated by the cyanobacteria *Oscillatoria* sp. and *S. platensis* showed antimicrobial properties when tested against pathogenic bacteria and fungi. As antibiotics and fungicides, both O.Ag_2O|AgO-NPs and S.Au-NPs demonstrated a strong synergistic impact. This may pave the door for a new generation of biological antimicrobial medications to combat multidrug-resistant bacteria and fungi.

Acknowledgements The authors are thankful to the Department of Botany and Microbiology, Faculty of Science, Menoufia University, Egypt, for providing scientific support to carry out this research work and support PhD thesis for L.H.S.Hassan. Thanks also to Prof. Mohamed T. Shabaan for his kind help and guidance during carrying this work.

Author contributions MME and HHM conceived and designed the structure of the article. MME, LHSH, and HHM performed the literature search and the data analysis. MME, LHSH, and HHM wrote the first draft of the manuscript. MME and HHM reviewed the manuscript. All authors read and approved the final version of the manuscript.

Funding The article received no funding.

Data availability Data sharing does not apply to this article as no datasets were generated or analyzed during the current study.

Declarations

Conflict of interest The authors declare no competing interests.

Ethics approval and consent to participate This article does not contain any studies with human participants or animals performed by any of the authors.

References

Adebayo-Tayo B, Ishola R, Oyewunmi T (2018) Characterization, antioxidant and immunomodulatory potential on exopolysaccharide produced by wild type and mutant *Weissella confusa* strains. Biotechnol Rep 19:271–278

Ahamad I, Aziz N, Zaki A, Zaki A, Fatma T (2021) Synthesis and characterization of silver nanoparticles using *Anabaena variabilis* as a potential antimicrobial agent. J Appl Phycol 33:829–841

Ali DM, Sasikala M, Gunasekaran M, Thajuddin N (2011) Biosynthesis and characterization of Sliver Nanoparticles using marine cyanobacterium, *Oscillatoria willel* NTDM01. Dig J Nanomater Biostruct 6(2):385–390

Al-Katib M, Al-Ahahri Y, Al-Niemi A (2015) Biosynthesis of silver nanoparticles by cyanobacterium *Gloeocapsa sp*. Intl J Enhanc Res Sci Technol Eng 4(9):60–73

Avilala J, Golla N (2019) Antibacterial and antiviral properties of silver nanoparticles synthesized by marine actinomycetes. Int J Pharmaceut Sci Res 10(3):1223–1228

Bakir E, Younis N, Mohamed M, El Semary N (2018) Cyanobacteria as nanogold factories: chemical and anti-myocardial infarction properties of gold nanoparticles synthesized by *Lyngbya majuscula*. Mar Drugs 16(6):217–237

Beyth N, Houri-Haddad Y, Domb A, Khan W, Hazan R (2015) Alternative antimicrobial approach: nano-antimicrobial materials. Evid Based Complement Alternat Med 2015:1–16

Corciova A, Ivanescu B (2018) Biosynthesis, characterization and therapeutic applications of plant-mediated silver nanoparticles. J Serb Chem Soc 83(5):515–538

Cui Y, Zhao Y, Tian Y, Zhang W, Lü X, Jiang X (2012) The molecular mechanism of action of bactericidal gold nanoparticles on *Escherichia Coli*. Biomaterials 33(7):2327–2333

Dananjaya SHS, Thao NT, Wijerathna HMSM, Lee J, Edussuriya M, Choi D, Kumar R (2020) *In vitro* and *in vivo* anticandidal efficacy of green synthesized gold nanoparticles using *Spirulina maxima* polysaccharide. Process Biochem 92:138–148

Dnyaneshwar KR, Mulani RM (2019) Biosynthesis of gold nanoparticles and its anti-*Candida albicans* activities. Ph.D. Thesis, Swami Ramanand Teerth Marathwada University, Nanded, India, pp 4

El-Seedi HR, El-Shabasy RM, Khalifa SAM, Saeed A, Shah A, Shah R, Iftikhar FJ, Abdel-Daim MM, Omri A, Hajrahand NH, Sabir JSM, Zou X, Halabi MF, Sarhann W, Guo W (2019) Metal nanoparticles fabricated by green chemistry using natural extracts: biosynthesis, mechanisms and applications. RSC Adv 9(42):24539–24559

El-Sheekh MM, El-Kassas HY (2014a) Application of biosynthesized silver nanoparticles against a cancer promoter cyanobacterium, *Microcystis aeruginosa*. Asian Pac J Cancer Prev 15(16):6773–6779

El-Sheekh MM, El-Kassas HY (2014b) Biosynthesis, characterization and synergistic effect of phytogenic gold nanoparticles by marine picoeukaryote *Picochlorum* sp. in combination with antimicrobials. Rend Fis Acc Lincei 25(4):513–521

El-Sheekh MM, El-Kassas HY (2016) Algal production of nano-silver and gold: their antimicrobial and cytotoxic activities: a review. J Genet Eng Biotechnol 14(2):299–310

El-Sheekh MM, Shabaan MT, Hassan L, Morsi HH (2020) Antiviral activity of algae biosynthesized silver and gold nanoparticles against Herps Simplex (HSV-1) virus *in vitro* using cell-line culture technique. Int J Environ Health Res. https://doi.org/10.1080/09603123.2020.1789946

El-Sheekh MM, Morsi HH, Hassan L (2021) Growth enhancement of *Spirulina platensis* through optimization of media and nitrogen sources. Egypt J Bot 61(1):61–69

Esmaeillou M, Zarrini G, Ahangarzadeh Rezaee M, Shahbazi mojarrad J, Bahadori A (2017) Vancomycin capped with silver nanoparticles as an antibacterial agent against multi-drug resistance bacteria. Adv Pharm Bull 7(3):479–483

González-Ballesteros N, Prado-Lopez S, Rodriguez-Gonzalez JB, Lastra M, Rodriguez-Arguelles MC (2017) Green synthesis of gold nanoparticles using brown algae *Cystoseira baccata*: its activity in colon cancer cells. Colloids Surf B Biointerfaces 153:190–198

Hamida RS, Abdelmeguid NE, Ali MA, Mohamed M, Bin-Meferij Khalil MI (2020) Synthesis of silver nanoparticles using a novel cyanobacteria *Desertifilum* sp. extract: their antibacterial and cytotoxicity effects. Int J Nanomedicine 15:49–63

Hamouda RA, Hussein MH, Abo-elmagd RA, Bawazir SS (2019) Synthesis and biological characterization of silver nanoparticles derived from the cyanobacterium *Oscillatoria limnetica*. Sci Rep 9(1):1–17

Husain S, Sardar M, Fatma T (2015) Screening of cyanobacterial extracts for synthesis of silver nanoparticles. World J Microbiol Biotechnol 31(8):1279–1283

Ismail GA, Ismail MM (2016) Comparative study of silver nanoparticles green biosynthesis using different seaweeds and their antimicrobial activity against some human pathogens. Ciência e Técnica Vitivinícola J 31(2):29–55

Jeffryes C, Agathos SN, Rorrer G (2015) Biogenic nanomaterials from photosynthetic microorganisms. Curr Opin Biotechnol 33:23–31

Jena J, Pradhan N, Dash BP, Lala BS, Prasanna KP (2013) Biosynthesis and characterization of silver nanoparticles using microalgae *Chlorococcum humicola* and its antibacterial activity. Int J Nanomater Biostruct 3(1):1–8

Kattarath SS, Ramani G (2017) Bioproduction and characterization of silver nanoparticles from microalgae *Asteracys quadricellulare*, its antimicrobial and antibiofilm activities. Int J Pharmacol Bio Sci 8(3):714–725

Khalafi T, Buazar F, Ghanemi K (2019) Phycosynthesis and enhanced photocatalytic activity of zinc oxide nanoparticles toward organosulfur pollutants. Sci Rep 9(1):1–10

Khalid M (2019) Nanotechnology and chemical engineering as a tool to bioprocess microalgae for its applications in therapeutics and bioresource management. Crit Rev Biotechnol 2019:1–18

Khan AU, Khan M, Malik N, Cho MH, Khan MM (2019) Recent progress of algae and blue–green algae-assisted synthesis of gold nanoparticles for various applications. Bioprocess Biosyst Eng 42(1):1–15

Khanna P, Kaur A, Goya D (2019) Algae-based metallic nanoparticles: synthesis characterization and applications: review. J Microbiol Meth 163:1–24

LewisOscar F, Vismaya S, Arunkumar M, Thajuddin N, Dhanasekaran D, Nithya C (2016) Algal nanoparticles: synthesis and biotechnological potentials Algae-organisms for imminent biotechnology, Chapter 7: pp 157–182

Mahdieh M, Zolanvari A, Azimee AS, Mahdieh M (2012) Green biosynthesis of silver nanoparticles by *Spirulina platensis*. Sci Iran 19(3):926–929

Maria BS, Devadiga A, Kodialbail VS, Saidutta MB (2015) Synthesis of silver nanoparticles using medical *Zizyphus xylopyrus* bark extract. Appl Nanosci 5:755–762. https://doi.org/10.1007/s13204-014-0372-8

Mata YN, Torres E, Blazquez ML, Ballester A, González F, Munoz JA (2009) Gold (III) biosorption and bioreduction with the brown alga *Fucus vesiculosus*. J Hazard Mater 166:612–618

Merin DD, Prakash S, Bhimba BV (2010) Antibacterial screening of silver nanoparticles synthesized by marine micro algae. Asian Pac J Trop Med 3(10):797–799

Mohammed HA, Abdel-Aziz MM, Hegazy MM (2019) Anti-oral pathogens of *Tecoma stans* (L.) and *Cassia javanica* (L.) flower volatile oils in comparison with chlorhexidine in accordance with their folk medicinal uses. Medicina 55(6):301–310

Morones JR, Elechiguerra JL, Camacho A, Holt K, Kouri JB, Ramírez JT, Yacaman MJ (2005) The bactericidal effect of silver nanoparticles. Nanotechnology 16(10):2346–2353

Moshfegh A, Jalali A, Salehzadeh A, Jozani AS (2019) Biological synthesis of silver nanoparticles by cell-free extract of *Polysiphonia* algae and their anticancer activity against breast cancer MCF-7 cell lines. Micro Nano Lett 14(5):581–584

Muthusamy G, Thangasamy S, Raja M, Chinnappan S, Kandasamy S (2017) Biosynthesis of silver nanoparticles from *Spirulina* microalgae and its antibacterial activity. Environ Sci Pollut Res 24(23):19459–19464

Nakamura S, Sato M, Sato Y, Ando N, Takayama T, Fujita M, Ishihara M (2019) Synthesis and application of silver nanoparticles (Ag-NPs) for the prevention of infection in healthcare workers. Int J Mol Sci 20(15):3620–3637

Negi S, Singh V (2018) Algae: a potential source for nanoparticle synthesis. J Appl Nat Sci 10(4):1134–1140

Pantidos N, Horsfall LE (2014) Biological synthesis of metallic nanoparticles by bacteria, fungi and plants. J Nanomed Nanotechnol 5(5):233–143

Parial D, Pal R (2015) Biosynthesis of monodisperse gold nanoparticles by green alga *Rhizoclonium* and associated biochemical changes. J Appl Phycol 27:975–984

Parial D, Patra HK, Roychoudhury P, Dasgupta AK, Pal R (2012) Gold nanorod production by cyanobacteria—a green chemistry approach. J Appl Phycol 24:55–60

Patel V, Berthold D, Puranik P, Gantar M (2015) Screening of cyanobacteria and microalgae for their ability to synthesize silver nanoparticles with antibacterial activity. Biotechnol Rep 5:112–119

Pathak J, Sonker AS, Rajneesh Singh V, Kumar D, Sinha RP (2019) Synthesis of silver nanoparticles from extracts of *Scytonema geitleri* HKAR-12 and their in vitro antibacterial and antitumor potentials. Litters Appl Nanobiosci 8(3):567–585

Poulose S, Panda T, Nair PP, Theodore T (2014) Biosynthesis of silver nanoparticles. J Nanosci Nanotechnol 14(2):2038–2049

Qing Y, Cheng L, Li R, Liu G, Zhang Y, Tang X, Wang J, Liu H, Qin Y (2018) Potential antibacterial mechanism of silver nanoparticles and the optimization of orthopedic implants by advanced modification technologies. Int J Nanomedicine 13:3311–3327

Rahman A, Kumar S, Nawaz T (2020) Chapter 17 - Biosynthesis of nanomaterials using algae. Microalgae cultivation for biofuels production, pp 265–279

Roh Y, Lauf RJ, McMillan AD, Zhang C, Rawn CJ, Bai J, Phelps TJ (2001) Microbial synthesis of metal-substituted magnetites. Solid State Commun 118:529–534

Senthilkumar P, Surendran L, Sudhagar B, Ranjith Santhosh Kumar DS (2019) Facile green synthesis of gold nanoparticles from marine algae *Gelidiella acerosa* and evaluation of its biological potential. SN Appl Sci 1:284

Sharma A, Sharma S, Sharma K, Chetri SPK, Vashishtha A, Singh P, Kumar R, Rathi B, Agrawal V (2015a) Algae as crucial organisms in advancing nanotechnology: a systematic review. J Appl Phycol 28(3):1759–1774

Sharma G, Jasuja ND, Kumar M, Ali MI (2015b) Biological synthesis of silver nanoparticles by cell-free extract of *Spirulina Platensis*. J Nanotechnol 2015:1–6

Soleimani M, Habibi-Pirkoohi M (2017) Biosynthesis of silver nanoparticles using *Chlorella vulgaris* and evaluation of the antibacterial efficacy against *Staphylococcus aureus*. Avicenna J Med Biotechnol 9(3):120–125

Sonker AS, Richa Pathak J, Rajneesh Kannaujia VK, Sinha RP (2017) Characterization and *in vitro* antitumor, antibacterial and antifungal activities of green synthesized silver nanoparticles using cell extract of *Nostoc* sp. strain HKAR-2. Canad J Biotechnol 1(1):26–37

Sudha S, Karthic RS, Rengaramanujam J (2013) Microalgae mediated synthesis of silver nanoparticles and their antibacterial activity against pathogenic bacteria. Ind J Exp Biol 52:393–399

Suganya KU, Govindaraju K, Kumar VG, Dhas TS, Karthick V, Singaravelu G, Elanchezhiyan M (2015) Blue green alga mediated synthesis of gold nanoparticles and its antibacterial efficacy against Gram positive organisms. Mater Sci Eng C 47:351–356

Suja CP, Lakshmana Senthil S, Anu Priya S, Shiny Preethi M, Renu A (2016) Optimization and characterization of silver nanoparticle synthesis from the microalgae, *Isochrysis galbana*. Biosci Biotechnol Res Commun 9(2):195–200

Tareq FK, Fayzunnesa M, Kabir MS (2017) Antimicrobial activity of plant-median synthesized silver nanoparticles against food and agricultural pathogens Microb Pathogen 109:228–232

Tunney MM, Ramage G, Field TR, Moriarty TF, Storey DG (2004) Rapid colorimetric assay for antimicrobial susceptibility testing of *Pseudomonas aeruginosa*. Antimicrob Agents Chemother 48(5):1879–1881

Vincy W, Mahathalana TJ, Sukumaran S, Jeeva S (2017) Algae as a source for synthesis of nanoparticles—a review. Int J Latest Trends Eng Technol 2017:5–9

Wei C, Li M, Zhao X (2018) Surface-enhanced Raman scattering (sers) with silver nano substrates synthesized by microwave for rapid detection of foodborne pathogens. Front Microbiol 9(2857):1–9

Yu Q, Li J, Zhang Y, Wang Y, Liu L, Li M (2016) Inhibition of gold nanoparticles (Au-NPs) on pathogenic biofilm formation and invasion to host cells. Sci Rep 6(1):1–14